

The Shape of the Correlation Function

Jakub Cimerman¹, Boris Tomášik², and Christopher Plumberg³

¹FNSPE, České vysoké učení technické v Praze, Břehová 7, 11519 Praha 1, Czechia;
jakub.cimerman@fjfi.cvut.cz

²Univerzita Mateja Bela, Tajovského 40, 97401 Banská Bystrica, Slovakia
and FNSPE, České vysoké učení technické v Praze, Břehová 7, 11519 Praha 1, Czechia;
boris.tomasik@cern.ch

³Department of Astronomy and Theoretical Physics, Lund University, Sölvegatan 14A,
SE-223 62, Lund, Sweden; christopher.plumberg@thep.lu.se

Abstract

The correlation function measured in ultrarelativistic nuclear collisions is non-Gaussian. By making use of models we discuss and assess how much various effects can influence its shape. In particular, we focus on the parametrisations expressed with the help of Lévy-stable distributions. We show that the Lévy index may deviate substantially from 2 due to non-critical effects such as non-spherical shape, resonance decays, event-by-event fluctuations and functional dependence on Q_{inv} or similar.

Keywords: correlation function; Lévy stable parametrisation; non-critical effects

1 Introduction

Correlation femtoscopy [1, 2] has become a standard technique for the experimental analysis of heavy-ion collisions. Usually, the two-particle correlation functions are fitted to a Gaussian form. However, the real shape of the correlation function is often strongly non-Gaussian and is often better described by a Lévy-stable distribution. A Lévy index much below 2 has recently been observed experimentally [3]. It has been suggested that even lower value of the Lévy index equal to 0.5 may identify matter produced at the critical endpoint of the QCD phase diagram. Despite this, there are some non-critical effects which can affect the value of the Lévy index significantly.

2 HBT Formalism

The two-particle correlation function probes the momentum-space structure of correlations between pairs of particles produced in heavy-ion collisions. In this work, we focus on correlations between charged pion pairs. The correlation function is constructed as the ratio of the two-particle spectrum to the product of two one-particle spectra, evaluated at momenta p_1 and p_2 :

$$C(p_1, p_2) = \frac{P_2(p_1, p_2)}{P(p_1)P(p_2)} = \frac{E_1 E_2 \frac{d^6 N}{dp_1^3 dp_2^3}}{\left(E_1 \frac{d^3 N}{dp_1^3}\right) \left(E_2 \frac{d^3 N}{dp_2^3}\right)}. \quad (1)$$

The correlation function is often expressed in terms of the momentum difference and the average momentum

$$q = p_1 - p_2, \quad K = \frac{1}{2}(p_1 + p_2). \quad (2)$$

The source of particle production can be described by the emission function $S(x, p)$ which describes the probability that a particle with momentum p is emitted from position x . The particle spectrum can then be calculated by integration of the emission function over the fireball volume.

Due to symmetrisation of the wave function of pairs of bosons, there is a peak in the correlation function for small q . Since we are interested in studying the region of the peak itself, we use the smoothness

approximation, where $K \approx p_1 \approx p_2$. Using this approximation the correlation function takes the form

$$C(q, K) - 1 \approx \frac{|\int d^4x S(x, K) e^{iqx}|^2}{(\int d^4x S(x, K))^2}. \quad (3)$$

The Gaussian parametrisation of the correlation function reads

$$C_G(\vec{q}, \vec{K}) = 1 + \lambda(\vec{K}) \exp \left[- \sum_{i,j=o,s,l} R_{ij}^2(\vec{K}) q_i q_j \right]. \quad (4)$$

Here, the HBT radii (in the out-side-long system) $R_{ij}^2(\vec{K})$ can be understood as lengthscales characterizing the homogeneity region which produces pion pairs with average momentum K , and λ quantifies the magnitude of the correlation function when $\vec{q} = 0$.

Nevertheless, since the Gaussian parametrisation often does not adequately describe the experimentally measured correlation function, we also use Lévy parametrisation of the correlation function

$$C_L(\vec{q}, \vec{K}) = 1 + \lambda'(\vec{K}) \exp \left[- \left| \sum_{i,j=o,s,l} R'_{ij}{}^2(\vec{K}) q_i q_j \right|^{\alpha/2} \right]. \quad (5)$$

The parameters λ' and $R'_{ij}{}^2$ are analogous to those used in the Gaussian parametrisation, but their values may differ from their Gaussian counterparts, and they also have no direct correspondence with the source widths often used to estimate and interpret the Gaussian R_{ij}^2 . The additional parameter α is known as the Lévy index and controls the form of the distribution used to approximate correlation function: for $\alpha = 2$ Lévy distribution becomes Gaussian distribution, while for $\alpha = 1$ it becomes exponential distribution.

When we use one-dimensional projection of relative momentum q , we also use a corresponding one-dimensional Lévy parametrisation

$$C_L(Q) = 1 + \lambda' \exp(-|R'Q|^\alpha). \quad (6)$$

3 Effects Leading to Non-Gaussianities

There are four effects we studied which can lead to non-Gaussianities. The first is event averaging. Each event possesses a variety of properties – such as size, geometric and dynamical anisotropies, and so on – which tend to fluctuate randomly from one event to the next. In order to build up statistics it is conventional to average correlation function over a large number of different events. The formula for the correlation function thus must be replaced by

$$C(q, K) \approx 1 + \frac{\left\langle |\int d^4x S(x, K) e^{iqx}|^2 \right\rangle_{\text{ev}}}{\left\langle (\int d^4x S(x, K))^2 \right\rangle_{\text{ev}}}. \quad (7)$$

Another way to improve statistical precision is to use a one-dimensional projection of the relative momentum. The correlation function is then a function of a single scalar quantity. There are two ways to perform this projection: either using Lorentz-invariant variable

$$Q_{\text{inv}}^2 = -q^\mu q_\mu = \vec{q} \cdot \vec{q} - (q^0)^2 \quad (8)$$

or a longitudinally boost-invariant one [3]

$$Q_{\text{LCMS}}^2 = \sqrt{(p_{1x} - p_{2x})^2 + (p_{1y} - p_{2y})^2 + q_{\text{long,LCMS}}^2}, \quad (9)$$

where $q_{\text{long,LCMS}}^2 = \frac{(p_{1z} E_2 - p_{2z} E_1)^2}{K_0^2 - K_l^2}$.

The next effect which can influence the shape of the correlation function is averaging with respect to the pair momentum \vec{K} . When measuring the correlation function bins in \vec{K} must be created which cannot be taken arbitrarily small. Thus the correlation function is averaged over some pair momentum interval which leads to an adjustment in the formula for the correlation function

$$C(q, K) \approx 1 + \frac{\int_{\text{bin}} d^3K |\int d^4x S(x, K) e^{iqx}|^2}{\int_{\text{bin}} d^3K (\int d^4x S(x, K))^2}. \quad (10)$$

The last effect we studied is the impact of resonance decays on the Lévy index. Different resonances contribute to the correlation function with different lengthscales and timescales, while the Gaussian function is given by only a single lengthscale. Therefore, the correlation function must deviate from a Gaussian form once resonance effects are included.

4 Models

To show that our results are not just model artifacts, we decided to use two different models. The first one is the blast-wave model [4], which describes an expanding locally thermalised fireball. It is characterized by the emission function

$$S(x, p)d^4x = \frac{m_t \cosh(\eta - Y)}{(2\pi)^3} d\eta dx dy \frac{\tau d\tau}{\sqrt{2\pi}\Delta\tau} \exp\left(-\frac{(\tau - \tau_0)^2}{2\Delta\tau^2}\right) \exp\left(-\frac{E^*}{T}\right) \Theta(1 - \bar{r}), \quad (11)$$

where $\Theta(1 - \bar{r})$ is Heaviside step function, $E^* = p_\mu p^\mu$ is the energy in the rest frame of the fluid and $\bar{r} = \frac{r}{R(\theta)}$ is a scaled radius of fireball in transverse plane. The blast-wave model also contains two types of anisotropies. Spatial anisotropy is characterized by a Fourier series in the azimuthal dependence of the fireball radius:

$$R(\theta) = R_0 \left(1 - \sum_{n=2}^{\infty} a_n \cos(n(\theta - \theta_n))\right). \quad (12)$$

Similarly, flow anisotropy reflects a distribution in the transverse rapidity:

$$\rho(\bar{r}, \theta_b) = \bar{r}\rho_0 \left(1 + \sum_{n=2}^{\infty} 2\rho_n \cos(n(\theta_b - \theta_n))\right). \quad (13)$$

To generate events we use DRAGON [5, 6], which is a Monte Carlo event generator based on the blast-wave model with added resonance decays. For this study we generated sets of 50,000 events with parameters set to: temperature $T = 120$ MeV, the average transverse radius $R_0 = 7$ fm, freeze-out time $\tau_{fo} = 10$ fm/c, the strength of the transverse expansion $\rho_0 = 0.8$, second order spatial anisotropy $a_2 \in (-0.1; 0.1)$ and second order flow anisotropy $\rho_2 \in (-0.1; 0.1)$. To calculate correlation functions from these events we used CRAB [7].

The second model we used is a hydrodynamical model of the collision system using iEBE-VISHNU [8, 9]. It is a 2+1-dimensional hydrodynamic simulation with boost-invariant Israel-Stewart hydrodynamics equations and Glauber Monte-Carlo initial conditions. For this study we generated 1,000 events of 0 – 10% Au+Au collisions at 200A GeV with a freeze-out temperature $T_{fo} = 120$ MeV and $\eta/s = 0.08$. To compute the HBT correlation function we used the HoTCoffeeh code [10], which directly evaluates Cooper-Frye integrals over the freeze-out surface on an event-by-event basis. Thanks to that we can calculate correlation functions with negligible uncertainties.

5 Results

Once we have the correlation functions, we can obtain the Lévy index with a 1D fit using Eq. (6) or a 3D fit using Eq. (5). In this study, we focus on the K_T -dependence of the Lévy index. First, we used the hydrodynamical model to check the relative importance of several of the effects discussed above. In Figure 1 we see the impact of three of these:

- correlation function with resonances (right panel) vs. without resonances (left panel),
- single event (solid blue and dashed green) vs. event-averaged (dotted red and dash-dotted cyan),
- Q_{inv} (solid blue and dotted red) vs. Q_{LCMS} (dashed green and dash-dotted cyan).

From this figure, we can say that the latter two effects do not affect the Lévy index significantly. For low K_T they shift α by less than 0.05. For high K_T , the impact is larger, but the shift is still much smaller than the one due to resonances. We find that the inclusion of resonances reduces the value of the Lévy index by 0.2-0.3. Nevertheless, as we show below, the largest effects are concentrated mainly at low K_T and are due to the use of a one-dimensional projection of the relative momentum.

Figure 2 shows the influence of averaging over various parameters of the blast-wave model. Events without averaging have fixed parameters $a_2 = 0.05$, $\rho_2 = 0.05$ and $\theta_2 = 0$, while events with averaging

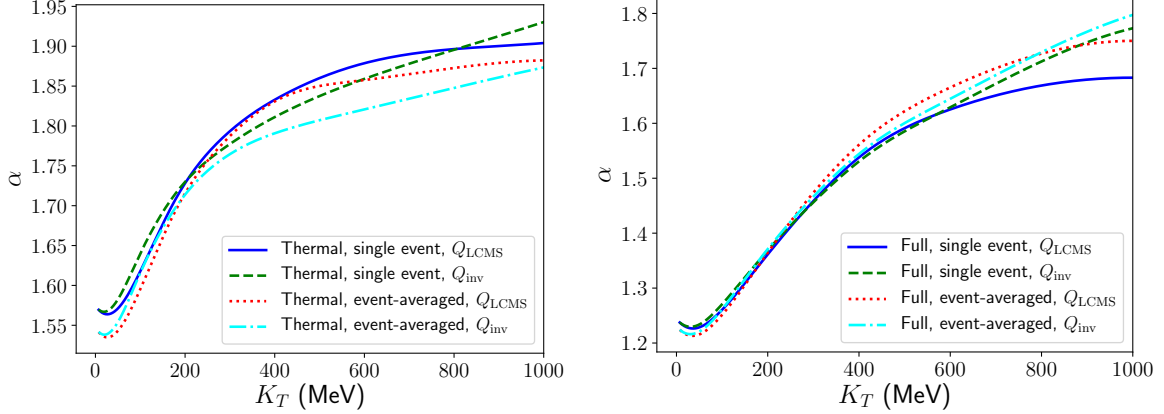


Figure 1: A comparison of $\alpha(K_T)$ with and without different non-Gaussian effects in hydrodynamic model: with and without event averaging and for different choices of Q (solid blue and dashed green vs. dotted red and dash-dotted cyan). The comparison is made both for thermal pions only (left panel) and for the full thermal and resonance contributions added together (right panel).

have those parameters running in interval $(-0.1; 0.1)$ for a_2 and ρ_2 , respectively $(0; 2\pi)$ for θ_2 . These plots show that the effect of averaging over a_2 is the biggest, but still smaller than the error bars. Thus we can say that this effect plays no role in the resulting value of the Lévy index.

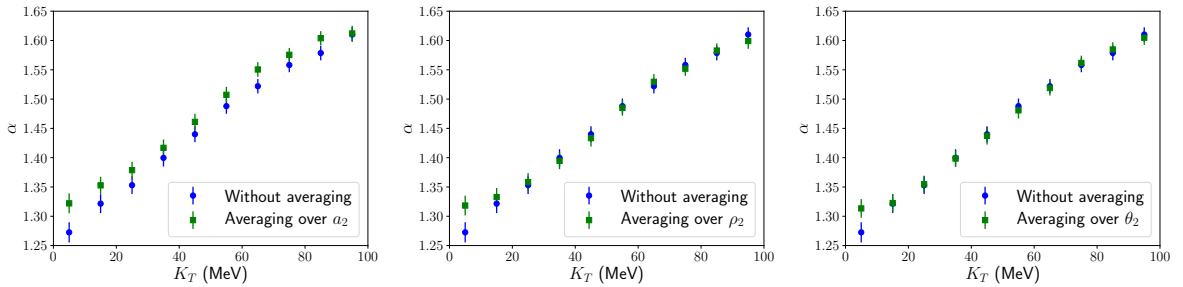


Figure 2: The Lévy index of the 1D fit to the correlation function in Q_{inv} . The green points show results calculated with fixed anisotropies, while the blue points show results calculated for averaged events over a_2 (left), ρ_2 (middle) and θ_2 (right).

To estimate the model-independent impact of resonances on the Lévy index, we calculated its K_T -dependences using both our models (Figure 3). This plot shows that, regardless of the model used in calculations, resonances reduce the value of the Lévy index by ~ 0.2 .

To find out why does the 1D projection affect Lévy index so significantly we have to look at the 3D correlation function. First, we fitted the correlation functions from both models in each direction separately. This is shown in Figure 4. These plots show, that while the correlation function behaves similar in outward and sideward direction, the K_T -dependence in longitudinal direction behaves differently. Moreover, it seems that the resonances do not affect the correlation function in the longitudinal direction as much as in the transverse plane.

To illustrate why the behaviour in different directions is so different, we plotted spatial distributions of the emission points of pions using the blast-wave model. Figure 5 shows us these profiles and we can see that even the source of pions along different axes looks unalike.

To use the whole 3D correlation function for obtaining the Lévy index, one can fit it with 3D Lévy distribution using Eq. (5). Such parametrisation is then fit to the correlation functions in all bins of q , not just along the axes. Figure 6 shows the K_T -dependence of the Lévy index obtained by a 3D fit of the correlation function. This figure underscores the fact that resonances can reduce the value of the Lévy index independently of the chosen model.

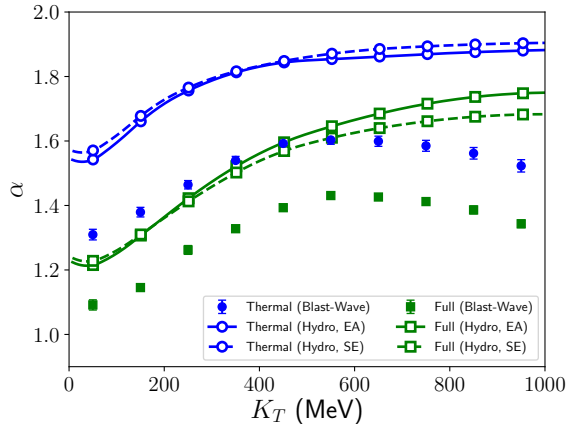


Figure 3: The Lévy index of the 1D fit to the correlation function in Q_{inv} . The blue circles show results from a source without resonances, while the green squares show results from a source with resonances. The solid points with error bars correspond to the blast-wave model and the open points represent the hydrodynamic results for event-averaged (solid) and single-event (dashed) correlation functions.

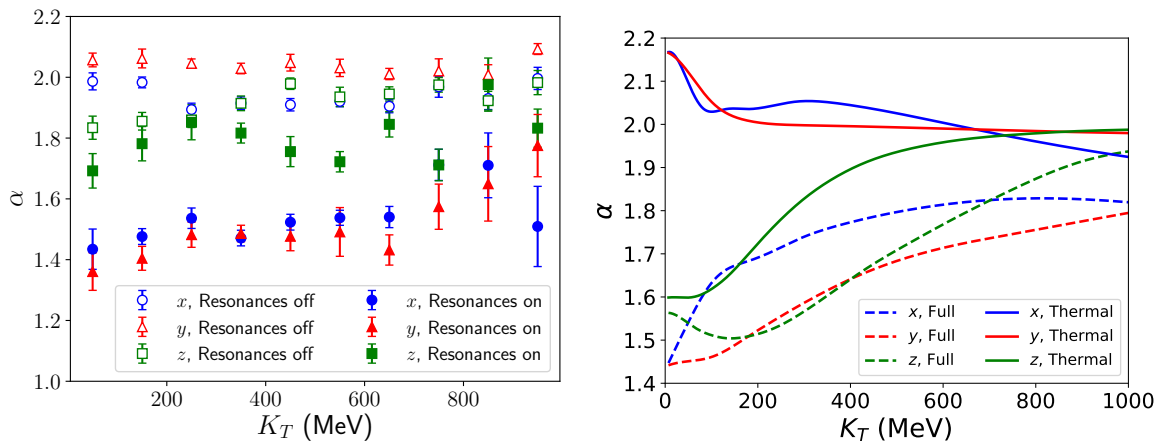


Figure 4: The Lévy index of the 1D fits to the correlation function in \vec{q} along different axes, with or without resonances. Left panel: blast-wave model. Right panel: hydrodynamics.

6 Conclusions

In this paper, we have shown that the shape of the correlation function, as well as the value of the Lévy index, may be influenced by a variety of different mechanisms. All our results show that the Lévy index may deviate substantially from the value of 2 due to non-critical effects. Some of these effects do not have significant influence, but others are found to cause notable deviations. The two most significant deviations arise, first, from the projection of the 3D relative momentum \vec{q} onto a scalar Q , and second, from the inclusion of resonance decays. Since we used two different models, these results appear to be robust and not merely artifacts of the models we have used. For this reason, the conclusions presented here may be regarded as model-independent.

Acknowledgements

This work was supported by the grant 17-04505S of the Czech Science Foundation (GAČR). BT also acknowledges support from VEGA 1/0348/18 (Slovakia). CP is funded by the CLASH project (KAW 2017-0036) and gratefully acknowledges the use of computing resources from both the Minnesota Supercomputing Institute (MSI) at the University of Minnesota and the Ohio Supercomputer Center [11] which contributed to the research results reported within this proceedings.

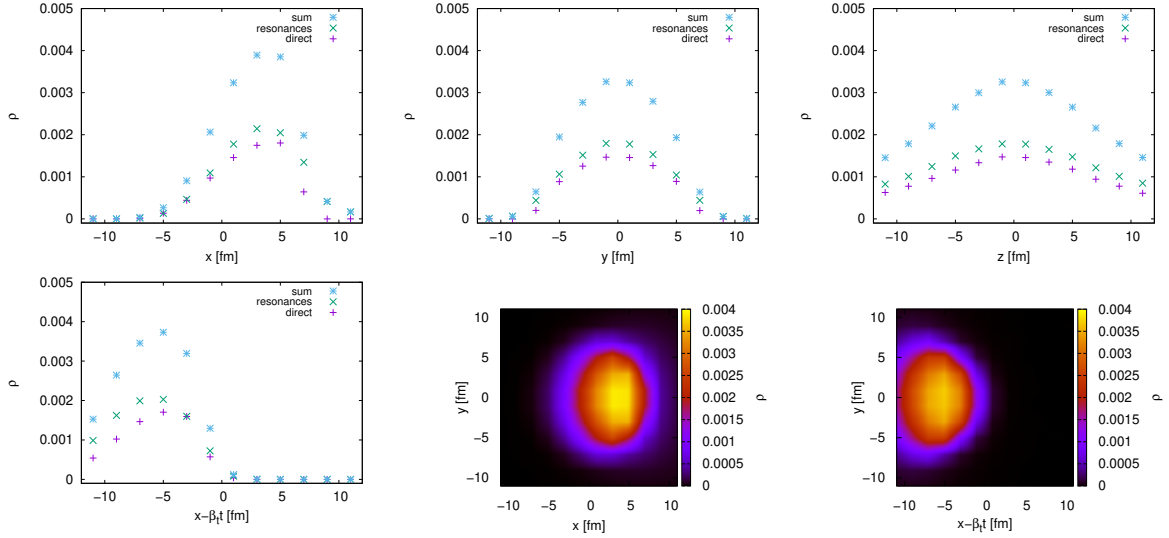


Figure 5: The spatial distribution of the emission points of pions. Upper row: the profiles of the emission points distribution along the x (left), y (middle), and z -axis (right). Lower row: the profile along the variable $(x - \beta_t t)$ (left), and two-dimensional distributions in the transverse plane (middle and right). The green \times 's show the profile of direct pions, the blue \star 's show the profile of pions produced by resonances and purple $+$'s show their sum. All these distributions were calculated as narrow integrals over the remaining coordinates with width 2 fm.

References

- [1] Heinz, U. and Jacak, B. V., Two-Particle Correlations in Relativistic Heavy-Ion Collisions, in *Ann. Rev. Nucl. Part. Sci.*, 1999, vol. 49, 529.
- [2] Lisa, M. A., Pratt, S., Soltz, R. and Wiedemann, U., Femtoscopy in Relativistic Heavy Ion Collisions: Two Decades of Progress, in *Ann. Rev. Nucl. Part. Sci.*, 2005, vol. 55, 357.
- [3] Adare, A, et al. (PHENIX collaboration), Lévy-stable two-pion Bose-Einstein correlations in $\sqrt{s_{NN}} = 200$ GeV Au+Au collisions, in *Phys. Rev. C*, 2018, vol. 97, 064911.
- [4] Retière, F. and Lisa, M. A., Observable implications of geometrical and dynamical aspects of freeze out in heavy ion collisions, in *Phys. Rev. C*, 2004, vol. 70, 044907.
- [5] Tomášik, B., DRAGON: Monte Carlo generator of particle production from a fragmented fireball in ultrarelativistic nuclear collisions, in *Comput. Phys. Commun.*, 2009, vol. 180, 1642.
- [6] Tomášik, B., DRoplet and hAdron generator for nuclear collisions: An update, in *Comput. Phys. Commun.*, 2016, vol. 207, 545.
- [7] Pratt, S., CoRelation After-Burner (CRAB), v3, available from <https://karman.physics.purdue.edu/oscar/repo/>
- [8] Song, H. and Heinz, U., Causal viscous hydrodynamics in 2 + 1 dimensions for relativistic heavy-ion collisions, in *Phys. Rev. C*, 2008, vol. 77, 064901.
- [9] Shen, C., Qiu, Z., Song, H., Bernhard, J., Bass, S. and Heinz, U., The iEBE-VISHNU code package for relativistic heavy-ion collisions, in *Comput. Phys. Commun.*, 2016, vol. 199, 61.
- [10] Plumberg, C. and Heinz, U., Hanbury-Brown–Twiss correlation functions and radii from event-by-event hydrodynamics, in *Phys. Rev. C*, 2018, vol. 98, no. 3, 034910.
- [11] Ohio Supercomputer Center. 1987. Ohio Supercomputer Center. Columbus OH: Ohio Supercomputer Center. <http://osc.edu/ark:/19495/f5s1ph73>.

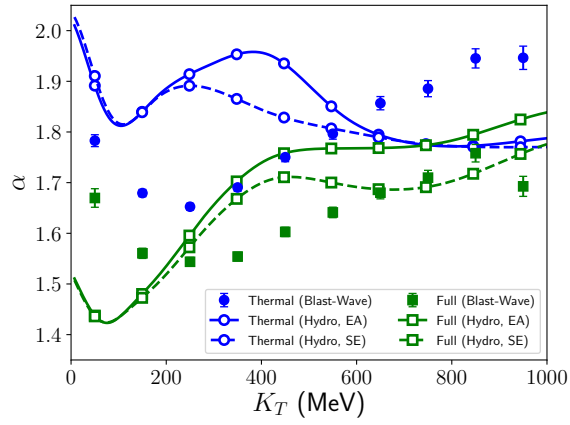


Figure 6: The Lévy index of the 3D fit to the correlation function according to Eq. (5), with and without resonances. The full points correspond to blast-wave model, while the empty points represent hydrodynamics. Solid lines connect points for the event-averaged correlation functions, while dashed lines correspond to the correlation function for a single event.